Dynamic Electrophoretic Mobility of Spherical Colloidal Particles in Realistic Aqueous Salt-Free Concentrated Suspensions

Félix Carrique,*,† Emilio Ruiz-Reina,‡ Francisco J. Arroyo,§ and Ángel V. Delgado||

Departamento de Física Aplicada I, Facultad de Ciencias, Universidad de Málaga, 29071 Málaga, Spain, Departamento de Física Aplicada II, Escuela Universitaria Politécnica, Universidad de Málaga, 29071 Málaga, Spain, Departamento de Física, Facultad de Ciencias Experimentales, Universidad de Jaén, 23071 Jaén, Spain, and Departamento de Física Aplicada, Facultad de Ciencias, Universidad de Granada, 18071 Granada, Spain

Received: March 15, 2010

In this contribution, the dynamic (or alternating current (AC)) electrophoretic mobility of spherical colloidal particles in a realistic salt-free concentrated suspension subjected to an oscillating electric field is studied theoretically using a cell model approach. Such a suspension is a concentrated one (in charged solid particles) in an aqueous solution without any electrolyte added during the preparation. The ionic species in solution can solely be: (i) the "added counterions" stemming from the particles (for example, by ionization of particle surface ionizable groups), (ii) the H^+ and OH^- ions from water dissociation, and (iii) the ions produced by the atmospheric CO_2 contamination. The corrections related to water dissociation and CO_2 contamination in suspensions open to the atmosphere have turned out to be tremendous in many of the experimental situations of interest in direct current (DC) electric fields. Thus, it is mandatory to explore their influence in the more complex situation of AC electrophoresis. The results confirm the importance of ions produced by water dissociation and those originated by the acidification of the aqueous solution in suspensions contaminated with atmospheric CO_2, for low to moderate particle volume fractions, where the role of the added counterions is screened by the other ionic species. It is worth mentioning that, for high particle charges, two Maxwell−Wagner processes develop in the mobility frequency spectrum, respectively linked to the diffuse layer relaxation and to the relaxation of a condensed layer of counterions located very close to the particle surface. This is the so-called ionic condensation effect for highly charged particles, already described in the literature, and which for the first time will be studied in detail in realistic salt-free systems. The dynamic electrophoretic mobility will be numerically computed throughout a wide frequency range and compared with the cases of pure and realistic salt-free conditions. In addition, the competition between different relaxation processes associated to the complex electric dipole moment induced on the particles by the field, the particle inertia, as well as their influence on the dynamic response, will be explored for pure and realistic cases.

1. Introduction

In recent years, a renewed interest has been dedicated to the study of electrokinetic phenomena in concentrated suspensions of charged particles, addressing both experimental and, mainly, theoretical aspects.[1–13] There is a particular case of special relevance due to the singular phenomenology it shows:[14] it is the case of the so-called salt-free concentrated suspensions. A pure or ideal salt-free suspension receives its name because it has no ions in solution different from those stemming from the particles themselves, related to the mechanism of particles charge generation. Because of the absence of external salts in solution, the electrostatic interactions between particles are weakly screened, thus forming short- or long-ranged ordered phases with phase transitions at relatively low volume fraction of particles. That is the reason they are usually called colloidal crystals or glasses.[14] Also, singular elastic behaviors associated with the overlapping of adjacent double layers, may favor the crystal ordering even at very low volume fractions.[15–19] On the other hand, one remarkable aspect that is magnified in salt-free suspensions is the counterion condensation effect, related to the compact layer of counterions that develops very close to the particle surface when the surface charge is sufficiently high.

Historically, the potential distribution around a spherical particle in a salt-free medium was originally investigated by Imai and Oosawa[20] and Oosawa,[21] for low particle concentration. In the past decade, different models have been derived concerning the electrokinetics of salt-free suspensions. First of all, we mention the excellent works by Ohshima dealing with aspects as the surface charge density-surface potential relationship,[22] stationary[23,24] and dynamic[25] electrophoretic mobilities, electrical conductivity, and sedimentation field.[26] These models studied the low particle concentration regime for some limiting analytical cases of low and high particle surface charge. More recently, Chiang et al.[27] extended Ohshima's model of the stationary salt-free electrophoretic mobility to arbitrary particle concentration. The present authors have also studied the direct current (DC) electrical conductivity and electrophoretic mobility in concentrated salt-free suspensions,[28] focusing mainly on the analysis of different electrohydrodynamic boundary conditions under a similar cell model approximation.[29–31] This approach was also

* Corresponding author. Address: Departamento de Física Aplicada I, Facultad de Ciencias, Universidad de Málaga, 29071 Málaga, Spain. E-mail: carrique@uma.es.
† Facultad de Ciencias, Universidad de Málaga.
‡ Escuela Universitaria Politécnica, Universidad de Málaga.
§ Universidad de Jaén.
|| Universidad de Granada.

10.1021/jp102350d
Published on Web 04/16/2010

used for the evaluation of the electroviscous effect in such suspensions.[32] In this contribution we develop a cell model for the dynamic electrophoretic mobility of particles in salt-free concentrated supensions, by considering for the first time realistic salt-free conditions.

It is important to point out the most relevant difference between salt-added and salt-free suspensions, namely, the absence of co-ions in the latter ones. When the dispersion medium is an electrolyte solution, the counterions stemming from the particles (the added counterions) are usually neglected due to their minor concentration as compared to those of counterions and co-ions of the external salt for typical conditions. However, the added counterions from the particles are the only ions present in a pure salt-free suspension. All the observed effects are unavoidably linked to such counterions, hence, the exact knowledge of their number and spatial distribution will be the first goal to achieve. On the other hand, an aqueous salt-free suspension necessarily has additional ions in solution coming from water dissociation, ions that can affect the ionic equilibrium in solution, particularly if one of them is the same ionic species as the added counterions. Moreover, in many situations the aqueous suspensions are open to the atmosphere and, inevitably, will have ions produced by the dissociation of the carbonic acid generated by the reaction of water with dissolved carbon dioxide. These new ionic species as well as those coming from water dissociation are extremely important when it comes to realistic salt-free systems for low to moderate particle concentrations. It is the importance of these effects in such suspensions that encouraged us to develop new general models accounting for them to help experimentalists to improve the comparison with real salt-free data in aqueous solutions. In a first step we derived a new double layer model for this kind of systems,[33] and studied the surface potential−surface charge relationship for different particle charges and volume fractions. From a quantitative point of view, the effects were tremendous for the lowest particle concentrations and highest particle charges. This scenario moved us immediately to address the DC electrokinetic response[34] and the electroviscous effect in realistic salt-free suspensions,[35] concluding once more the large influence that the latter effects have on the response of a salt-free suspension. As these phenomena were explored, the numerical problems increasingly grew due to the more complex picture associated with the now integro-differential Poisson−Boltzmann equation to account for the coupling between added counterions and particle charge.

In the present paper we study the dynamic mobility of a spherical particle in the presence of an oscillating electric field. Serious numerical problems have been solved due to the stiff nature of the general electrokinetic equations as the frequency of the applied electric field increases approaching the gigahertz region, where water molecules start to relax (this dielectric relaxation is out of the frequency range of validity of our model). The necessity of perfectly knowing the coupling between all ionic species present in the system through their chemical reactions in solution considerably complicates the ideal salt-free picture. This paper is devoted to that goal for the alternating current (AC) regime. Thus, in the following sections we will show calculations of the dynamic electrophoretic mobility as a function of frequency for different particle charges and volume fractions, always comparing between pure and realistic predictions.

2. Theory

Electrokinetic Equations and Boundary Conditions. The electrokinetic equations and boundary conditions for the general case of concentrated suspensions in alternating electric fields under the cell model approximation are well-known.[12,36,37] In order to facilitate the reading and further analysis, we will briefly show the most important theoretical aspects.

According to Kuwabara's cell model,[38] each spherical particle of radius a is located at the center of a spherical shell of solution of radius b such that the particle/cell volume ratio in the unit cell is equal to the particle volume fraction ϕ throughout the whole suspension, i.e.,

$$\phi = (a/b)^3 \tag{1}$$

Particle−particle electro-hydrodynamic interactions in concentrated suspensions are handled through appropriate boundary conditions at the outer surface of the cell. The particle bears a surface charge density σ, and it is immersed in an aqueous solution of relative permittivity ϵ_{rs}, mass density ρ_s and viscosity η_s, containing added counterions of valence z_1 and drag coefficient λ_1, and other ionic species that we will relate to water dissociation and CO_2 contamination with an index j ($j = 2,..,n$), with valences z_j and drag coefficients λ_j. The amount of added counterions in solution exactly counterbalances the charge on the particles. If an alternating electric field $\mathbf{E}e^{-i\omega t}$ of angular frequency ω is applied to the suspension, each particle will move with an electrophoretic velocity $\mathbf{v}_e e^{-i\omega t}$. The reference system is fixed to the particle's center, being the polar axis ($\theta = 0$) parallel to the electric field. The fundamental equations connecting electrical potential $\Psi(\mathbf{r},t)$, the number density of ions $n_j(\mathbf{r},t)$, their drift velocity $\mathbf{v}_j(\mathbf{r},t)$, the fluid velocity $\mathbf{v}(\mathbf{r},t)$, and the pressure $P(\mathbf{r},t)$ are[7,39–42]

$$\nabla^2\Psi(\mathbf{r},t) = -\frac{\rho_{el}(\mathbf{r},t)}{\varepsilon_{rs}\varepsilon_0} \tag{2}$$

$$\rho_{el}(\mathbf{r},t) = \sum_{j=1}^{n} z_j e n_j(\mathbf{r},t) \tag{3}$$

$$\eta_s\nabla^2\mathbf{v}(\mathbf{r},t) - \nabla P(\mathbf{r},t) - \rho_{el}(\mathbf{r},t)\nabla\Psi(\mathbf{r},t) = \rho_s\frac{\partial}{\partial t}[\mathbf{v}(\mathbf{r},t) + \mathbf{v}_e\exp(-i\omega t)] \tag{4}$$

$$\nabla\cdot\mathbf{v}(\mathbf{r},t) = 0 \tag{5}$$

$$\mathbf{v}_j(\mathbf{r},t) = \mathbf{v}(\mathbf{r},t) - \frac{1}{\lambda_j}\nabla\mu_j(\mathbf{r},t) \quad (j = 1,...,n) \tag{6}$$

$$\mu_j(\mathbf{r},t) = \mu_j^\infty + z_j e\Psi(\mathbf{r},t) + k_B T\ln n_j(\mathbf{r},t) \quad (j = 1,...,n) \tag{7}$$

$$\nabla\cdot\sum_{j=1}^{n}[z_j e n_j(\mathbf{r},t)\mathbf{v}_j(\mathbf{r},t)] = -\frac{\partial}{\partial t}[\rho_{el}(\mathbf{r},t)] \tag{8}$$

where e is the elementary electric charge, k_B is Boltzmann's constant, T is the absolute temperature, and $\mu_j(\mathbf{r},t)$ is the chemical potential of the jth ionic species, with μ_j^∞ being its standard

value. Equation 2 is Poisson's equation, where $\rho_{el}(\mathbf{r},t)$ is the electric charge density given by eq 3. Equations 4 and 5 are the Navier−Stokes equations for an incompressible fluid flow at low Reynolds number in the presence of an electrical body force. Equation 6 means that the ionic flow is due in part to both the liquid flow and the gradient of the electrochemical potential defined in eq 7. The drag coefficient λ_j in eq 6 is related to the limiting ionic conductance Λ_j^0 or the diffusion coefficient D_j by[39]

$$\lambda_j = \frac{N_A e^2 |z_j|}{\Lambda_j^0} = \frac{k_B T}{D_j} \quad (j = 1, ..., n) \tag{9}$$

where N_A is Avogadro's number.

An important difference between realistic and pure salt-free suspensions is represented by the continuity eq 8. It stands for total charge conservation instead of conservation of the number of every individual ionic species in the system. This is required by the fact that chemical reactions are present, and the subsequent ionic coupling precludes conservation of the number concentration of individual species. If the added counterions were different from those associated with water dissociation and CO_2 contamination, we can use a continuity equation for the conservation of the number of just the added counterions, in addition to the charge conservation eq 8. We also assume that the chemical reactions in the solution are faster than any other ionic processes in response to the electric field, so as to ensure that the chemical local equilibrium is attainable everywhere in the suspension.

We still need more equations to completely solve the problem. For that purpose, and as a first approximation, an equilibrium scheme for chemical reactions will be followed, and their mass-action equations will be used locally in addition to the general system of eqs 2−8. Using a linear perturbation scheme, each quantity X is written as the sum of its equilibrium value, X^0, plus a perturbation term δX linearly dependent with the field and with its same time dependence:

$$\begin{aligned}
&\Psi(\mathbf{r},t) = \Psi^0(r) + \delta\Psi(\mathbf{r})e^{-i\omega t}\\
&n_j(\mathbf{r},t) = n_j^0(r) + \delta n_j(\mathbf{r})e^{-i\omega t} \quad (j = 1,...,n)\\
&\mu_j(\mathbf{r},t) = \mu_j^0 + \delta\mu_j(\mathbf{r})e^{-i\omega t} (j = 1,...,n)\\
&P(\mathbf{r},t) = P^0(r) + P(\mathbf{r})e^{-i\omega t}\\
&\mathbf{v}(\mathbf{r},t) = \mathbf{v}(\mathbf{r})e^{-i\omega t}\\
&\mathbf{v}_j(\mathbf{r},t) = \mathbf{v}_j(\mathbf{r})e^{-i\omega t} \quad (j = 1,...,n)\\
&\rho_{el}(\mathbf{r},t) = \rho_{el}^0(r) + \delta\rho_{el}(\mathbf{r})e^{-i\omega t}
\end{aligned} \tag{10}$$

with $r = |\mathbf{r}|$.

The equilibrium volume charge density is given by

$$\rho_{el}^{(0)}(r) = \sum_{j=1}^{n} z_j e n_j^{(0)}(r) \tag{11}$$

and the equilibrium ionic concentration

$$n_j^{(0)}(r) = b_j \exp\left(-\frac{z_j e\Psi^{(0)}(r)}{k_B T}\right) \quad (j = 1, ..., n) \tag{12}$$

obeys the Boltzmann distribution. The quantities b_j ($j = 1$, ..., n) represent the concentration of the respective ions at the position of zero equilibrium electrical potential. This is chosen at the outer surface of the cell

$$\Psi^{(0)}(b) = 0 \tag{13}$$

For the special case in which the added counterions ($j = 1$) are different from any other ionic species in realistic salt-free suspensions, the electroneutrality of the cell imposes the condition

$$\int_a^b n_1^{(0)}(r)4\pi r^2\,dr = \int_a^b b_1 \exp\left(-\frac{z_1 e\Psi^{(0)}(r)}{k_B T}\right)4\pi r^2\,dr = \frac{-4\pi a^2\sigma}{z_1 e} \tag{14}$$

In this case, the Poisson−Boltzmann equation becomes integro-differential,

$$\frac{1}{r^2}\frac{d}{dr}\left(r^2\frac{d\Psi^{(0)}}{dr}\right) = -\frac{1}{\varepsilon_{rs}\varepsilon_0}\sum_{j=1}^{n} z_j e n_j^{(0)}(r) \tag{15}$$

with

$$n_1^{(0)}(r) = \frac{(-4\pi a^2\sigma)\exp\left(-\frac{z_1 e\Psi^{(0)}(r)}{k_B T}\right)}{z_1 e\int_a^b \exp\left(-\frac{z_1 e\Psi^{(0)}(r)}{k_B T}\right)4\pi r^2\,dr} \tag{16}$$

and the boundary conditions are expressed by eq 14 and

$$\frac{d\Psi^{(0)}}{dr}(b) = 0 \tag{17}$$

or, alternatively, by eq 17 and

$$\frac{d\Psi^{(0)}}{dr}(a) = -\frac{\sigma}{\varepsilon_{rs}\varepsilon_0} \tag{18}$$

after application of Gauss theorem and consideration of the electroneutrality of the cell. The rest of the unknowns b_j ($j = 2,...,n$) can be obtained from the equations representing the equilibrium chemical reactions in solution for the ionic species involved. An interested reader can find in ref 33 a complete study of all the possible cases and the methods of resolution of the resulting integro-differential Poisson−Boltzmann equations.

The symmetry of the problem allows us to define the functions $h(r)$, $\phi_j(r)$ ($j = 1,...,n$) and $Y(r)$, as[5]

$$\mathbf{v}(\mathbf{r}) = (v_r, v_\theta, v_\varphi) = \left(-\frac{2}{r}hE\cos\theta, \frac{1}{r}\frac{\mathrm{d}}{\mathrm{d}r}(rh)E\sin\theta, 0\right) \quad (19)$$

$$\delta\Psi(\mathbf{r}) = -Y(r)E\cos\theta \quad (20)$$

$$\delta\mu_j(\mathbf{r}) = z_j e\delta\Psi + k_B T\frac{\delta n_j}{n_j^0} = -z_j e\phi_j(r)E\cos\theta \quad (j = 1, ..., n) \quad (21)$$

with $E = |\mathbf{E}|$.

Applying the procedure in eq 10 and eqs 19−21 to the basic differential equations 2−8, we obtain, after neglecting nonlinear perturbations terms

$$L(Lh + \gamma^2 h) = -\frac{e}{\eta_s r}\frac{\mathrm{d}y}{\mathrm{d}r}\sum_{j=1}^{n} b_j z_j^2 \mathrm{e}^{-z_j y}\phi_j(r) \quad (22)$$

$$\sum_{j=1}^{n}\frac{z_j^2 e^2 n_j^{(0)}(r)}{\lambda_j}\left\{L\phi_j(r) - \frac{\mathrm{d}y}{\mathrm{d}r}\left(z_j\frac{\mathrm{d}\phi_j}{\mathrm{d}r} - \frac{2\lambda_j}{e}\frac{h(r)}{r}\right) - \frac{i\omega\lambda_j}{k_B T}[Y(r) - \phi_j(r)]\right\} = 0 \quad (23)$$

$$LY(r) = \sum_{j=1}^{n}\frac{z_j^2 e^2 n_j^0(r)}{\varepsilon_{rs}\varepsilon_0 k_B T}[Y(r) - \phi_j(r)] \quad (24)$$

where

$$y = \frac{e\Psi^0}{k_B T} \quad (25)$$

$$\gamma = \sqrt{\frac{i\omega\rho_s}{\eta_s}} = (i+1)\sqrt{\frac{\omega\rho_s}{2\eta_s}} \quad (26)$$

$$L \equiv \frac{\mathrm{d}^2}{\mathrm{d}r^2} + \frac{2}{r}\frac{\mathrm{d}}{\mathrm{d}r} - \frac{2}{r^2} \quad (27)$$

The boundary conditions are

$$\Psi_p(\mathbf{r}) = \Psi(\mathbf{r}) \text{ at } r = a \quad (28)$$

$$\varepsilon_{rs}\nabla\Psi(\mathbf{r})\cdot\hat{\mathbf{r}} - \varepsilon_{rp}\nabla\Psi_p(\mathbf{r})\cdot\hat{\mathbf{r}} = -\sigma/\varepsilon_0 \text{ at } r = a \quad (29)$$

$$\mathbf{v} = 0 \text{ at } r = a \quad (30)$$

$$\mathbf{v}_j\cdot\hat{\mathbf{r}} = 0 \text{ at } r = a \quad (j = 1, ..., n) \quad (31)$$

$$v_r = -\mathbf{v}_e\cdot\hat{\mathbf{r}} \text{ at } r = b \quad (32)$$

$$\boldsymbol{\omega} = \nabla\times\mathbf{v} = \mathbf{0} \text{ at } r = b \quad (33)$$

where $\Psi_p(\mathbf{r})$ is the electrical potential in the interior region of the solid particle and ε_{rp} is its relative permittivity. Equation 28 expresses the continuity of the electrical potential at the surface of the particle. Equation 29 relates the discontinuity of the normal component of the electrical displacement vector with the particle charge density, where $\hat{\mathbf{r}}$ is the normal vector outward to the surface. Equation 30 means that the liquid cannot slip on the particle. Due to the nonconducting nature of the particle, the velocity of ions in the normal direction to the particle surface is zero (eq 31). In the outer surface of the cell ($r = b$), we will follow Kuwabara's boundary conditions. In the radial direction, the velocity of the liquid will be minus the radial component of the electrophoretic velocity, as expressed by eq 32, and, finally, eq 33 means that the liquid flow is free of vorticity on that surface.

Analogously to eq 20, the inner electrical potential perturbation can be expressed by

$$\delta\Psi_p(\mathbf{r}) = -Y_p(r)E\cos\theta \quad (34)$$

According to symmetry considerations, the latter boundary conditions transform into

$$h(a) = 0, \quad \frac{\mathrm{d}h}{\mathrm{d}r}(a) = 0 \quad (35)$$

$$Lh(b) = 0 \quad (36)$$

$$u_e = \frac{2h(b)}{b} \quad (37)$$

$$\frac{\mathrm{d}\phi_j}{\mathrm{d}r}(a) = 0 \quad (j = 1, ..., n) \quad (38)$$

$$\frac{\mathrm{d}Y}{\mathrm{d}r}(a) - \frac{\varepsilon_{rp}}{\varepsilon_{rs}}\frac{Y(a)}{a} = 0 \quad (39)$$

In addition, considering the equation of motion for the unit cell,[43] we have

$$\frac{\mathrm{d}^3 h}{\mathrm{d}r^3}(b) + \frac{1}{b}\frac{\mathrm{d}^2 h}{\mathrm{d}r^2}(b) - \frac{6}{b^2}\frac{\mathrm{d}h}{\mathrm{d}r}(b) + \frac{6}{b^3}h(b) - \frac{i\omega\rho_s}{\eta_s}\left[\frac{h(b)}{b} - u_e\frac{(\rho_p - \rho_s)}{\rho_s}\phi - \frac{\mathrm{d}h}{\mathrm{d}r}(b)\right] = \frac{\rho_{el}^0(b)\mathrm{Y}(b)}{b\eta_s} \quad (40)$$

where u_e is the dynamic mobility relating the electrophoretic velocity $\mathbf{v}_e$ to the macroscopic experimentally measured electric field $\mathbf{E}$, as follows:

$$\mathbf{v}_e\exp(-i\omega t) = u_e\mathbf{E}\exp(-i\omega t) \quad (41)$$

According to the Shilov−Zharkikh cell model,[29] the connection between the macroscopic field $\mathbf{E}$ and local electrical properties is expressed as

$$\delta\Psi(\mathbf{r})|_{r=b} = -Eb\cos\theta \quad (42)$$

This can be written, by using the function $Y(r)$, as

$$Y(b) = b \quad (43)$$

Although other choices can be proposed, this boundary condition for the electric potential perturbation has been used by most authors working with electrokinetic cell models.[11,27,44–47] In addition, a boundary condition is also required for the ionic perturbation at the outer surface of the cell:[29]

$$\delta n_j(b) = 0 \quad (j = 1, ..., n) \tag{44}$$

or, making use of the spherical symmetry,

$$\phi_j(b) = Y(b) \quad (j = 1, ..., n) \tag{45}$$

In ref 48 it has been shown that this choice leads to results in very good agreement with experimental data.

Dynamic Electrophoretic Mobility. Because the equilibrium electrical potential $\Psi^{(0)}(r)$ explicitly appears in the differential electrokinetic equations, the first step in our derivation is solving the equilibrium Poisson−Boltzmann equation for the cases of interest. A full description of the mathematical details can be found in a recent contribution from the authors.[11]

It must be mentioned that the dynamic mobility described above is valid if the fluid velocity is related to a reference frame fixed to the particle, and hence, the liquid is at rest far from the particle in the laboratory reference frame. However, some experimental devices for the determination of u_e require that the mobility be referred to the center-of-mass system, characterized by the zero value of the macroscopic momentum per unit volume represented as the volume average $\langle \rho \mathbf{u_L} \rangle$ in the cell, where ρ and $\mathbf{u_L}$ are, respectively, the local mass density and velocity with respect to the laboratory frame.[49,50] In a previous work we addressed that issue, obtaining the following expression for the dynamic mobility in the zero-momentum frame:[50]

$$u_e = \frac{2h(b)}{b} \frac{1}{\left[1 + \left(\frac{\rho_p - \rho_s}{\rho_s}\right)\phi\right]} \tag{46}$$

For the cases considered in this paper ($\rho_p = 1057$ kg·m^{-3}; $\rho_s = 997$ kg·m^{-3};$\phi \leq 0.5$), the maximum correction factor multiplying $2h(b)/b$ is roughly 0.97 for $\phi = 0.5$, and therefore, the data presented in the following will not be corrected. It has to be mentioned that other recent electrokinetic cell models valid for concentrated suspensions[37] in salt solutions use some of the previous boundary conditions, justifying them on well-founded physical grounds instead of using the more "ad hoc" procedure of the present model. However, it can be shown that both approaches lead to exactly the same results.

Turning back to concentrated salt-free suspensions, our main aim is to analyze the predictions of the present model once the realistic considerations of water dissociation and CO_2 contamination are incorporated into the theory. As the changes experienced by the mobility in DC electric fields are quite important[34] (a significant diminution of its value at low to moderate particle volume fractions and high surface charges as compared to pure or ideal salt-free predictions), we also aim to explore the influence of the realistic corrections in the case of the dynamic mobility for the whole frequency range of validity of the model (from DC to GHz). It will be shown that these effects cannot be neglected in many experimental conditions, thus improving the comparison with experiments.

Realistic Corrections to the Dynamic Electrophoretic Mobility: Water Dissociation and CO_2 Contamination. Let us first assume that there are H^+ and OH^- ions coming from water dissociation in the aqueous solution in addition to the added counterions. In such scenario we could distinguish between the cases: (a) the added counterions coincide with H^+ or OH^- ions (number of different ionic species $n = 2$), and (b) they are all different ionic species ($n = 3$). This distinction is quite relevant because, in the former case, the added counterions will enter the reaction equation for water dissociation, whereas in case b they do not. The second step in realistically describing salt-free systems deals with the consideration of ions stemming from the atmospheric CO_2 contamination in the aqueous medium. Again, we can distinguish between two cases: (a) when the added counterions are coincident with one of the ionic species in the system (H^+, OH^-, HCO_3^- ions) ($n = 3$), thus entering in one of the equilibrium dissociation equations, and (b) when they are all different ($n = 4$). For both realistic cases, the water dissociation reaction $H_2O \rightleftarrows H^+ + OH^-$ is taken into account. For the second one, the following equilibria will also be considered:

$$\begin{aligned} CO_2 + H_2O &\rightleftarrows H_2CO_3 \\ H_2CO_3 &\rightleftarrows H^+ + HCO_3^- \\ HCO_3^- &\rightleftarrows H^+ + CO_3^{=} \end{aligned} \tag{47}$$

As it was already reported,[11] the role of the divalent $CO_3^{=}$ ions can be neglected because of the lower equilibrium constant of their chemical dissociation reaction.

The Frequency Variation of the Dynamic Mobility. It is worth recalling that, at low frequency, say below 1 kHz, the motion of the particle in an ordinary salt-added solution is the result of

i. The action of the applied field on its net charge.

ii. The viscous friction of the liquid.

iii. The motion of the charged liquid surrounding it (the liquid inside the double layer) under the action of external and local fields.

iv. The field generated by the dipole moment induced on the particle and its double layer by the applied electric field. The larger the dipole moment, the smaller the mobility. Here we have electromigration contributions (the field accumulates counterions on one side of the particle and depletes them on the other side) and diffusive ones. For suspensions in salt solutions, the latter are basically due to the formation of an electrolyte concentration gradient (concentration polarization) because of the different transport numbers of ions inside and outside the double layer.

As the frequency is increased from zero, a critical value (the α-relaxation frequency ω_α) is reached for which the concentration polarization cannot occur. As a consequence, the induced dipole moment increases and the mobility decreases.[50] At still higher frequency (the Maxwell−Wagner (MW) relaxation frequency, ω_{MW}, typically in the megahertz range) the ions cannot follow the fast field oscillations, hence the dipole moment decreases, and the mobility rises. Finally, the frequency can be so high (the inertial relaxation, ω_i) that the inertia of the particle and fluid hinder any motion, and the mobility shows a continuous decline as the frequency increases. Approximate expressions for these characteristic frequencies are, in the case of dilute systems in salt solutions,

$$\omega_\alpha = \frac{2D}{a^2}$$
$$\omega_{MW} = \frac{(1-\phi)\kappa_p + (2+\phi)\kappa_s}{(1-\phi)\varepsilon_{rp}\varepsilon_0 + (2+\phi)\varepsilon_{rs}\varepsilon_0} \quad (48)$$
$$\omega_i = \frac{\eta_s}{\rho_s a^2}$$

where D is an effective diffusion coefficient,[51] κ_s is the medium conductivity, and the particle (assumed to be made of a nonconducting material) conductivity κ_p will be exclusively associated to its surface conductivity, κ^σ, due to the presence of an excess of counterions in the ionic atmosphere[51] ($\kappa_p = 2\kappa^\sigma/a$).

In the case of salt-free systems, the inertial processes are obviously the same as described, and can be expected to occur at the same frequencies, considering that such processes should not depend on either surface charge or volume fraction. In addition, a simple Maxwell−Wagner relaxation process must also exist in salt-free suspensions for similar reasons as those already stated. Ions can only migrate along very short distances if the period of the field is below their characteristic times for electromigration and diffusion.

The new feature appearing in pure salt-free systems is the absence of co-ions, and we can wonder about the existence or not of the α-relaxation because no neutral electrolyte concentration gradients can be developed. This will be considered below.

3. Results and Discussion

General Features of the Mobility Frequency Dependence in Salt-Free Systems. The electrophoretic mobility u_e of a spherical particle in a concentrated colloidal suspension can be obtained from eq 37. As usual, the mobility data will be made dimensionless as follows:

$$u_e^* = \frac{3\eta_s e}{2\varepsilon_{rs}\varepsilon_0 k_B T} u_e \quad (49)$$

Figure 1 shows the modulus and phase of the dimensionless dynamic mobility for low volume fractions of particles in the three salt-free cases: pure salt-free (SF), realistic salt-free considering water dissociation (SFW), and realistic salt-free with water dissociation and effects of the atmospheric CO_2 contamination (SFWC). Results corresponding to four widely separated particle charge densities have been included. It is first of all noticeable that increasing the ionic content in the medium, because of water or CO_2-related ions, leads to a decrease of the low frequency mobility. This is in agreement with our previous results in DC fields,[34] and it can be explained by the larger screening effect associated with the higher ionic strength. As surface charge increases, so does the low frequency mobility, although the variation is not at all monotonous: compare the differences between the mobilities at −0.01 and −0.1 μC/cm^2 (five mobility units increase), and at −1 and −10 μC/cm^2 (less than 0.5 units in mobility). This means that the electrokinetically mobile charge reaches some sort of saturation, perfectly explainable in terms of the counterion condensation effects.[23,27,28]

As it is well-known, this consists of the accumulation of counterions in a region very close to the particle surface, occurring above some critical value of the surface charge density. In such conditions, both the mobility and the electric potential change very little with a further increase of the surface

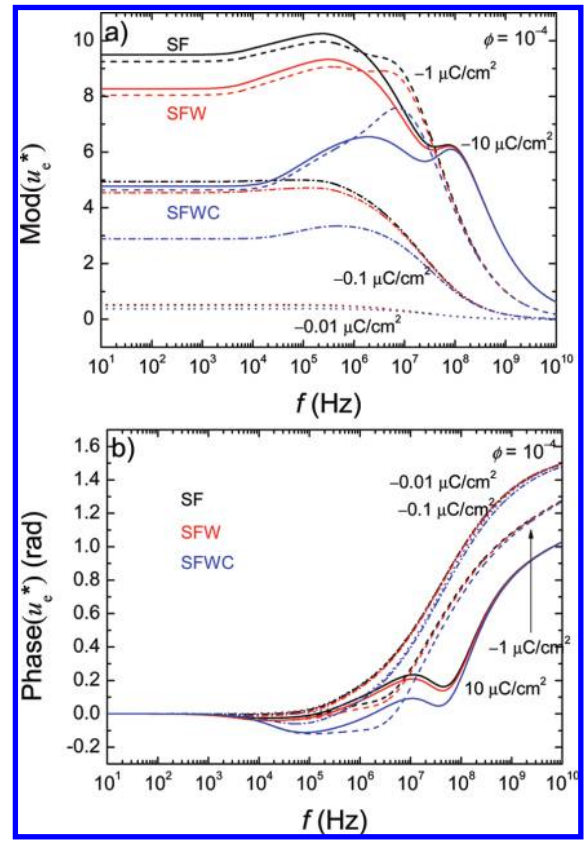

Figure 1. Modulus (a) and phase (b) of the dimensionless dynamic electrophoretic mobility of a spherical particle in a pure SF suspension, and in realistic salt-free suspensions, SFW and SFWC, at 25 °C as a function of frequency. The surface charge densities σ are indicated. Volume fraction: $\phi = 0.0001$; particle radius: $a = 100$ nm; added counterions: H^+.

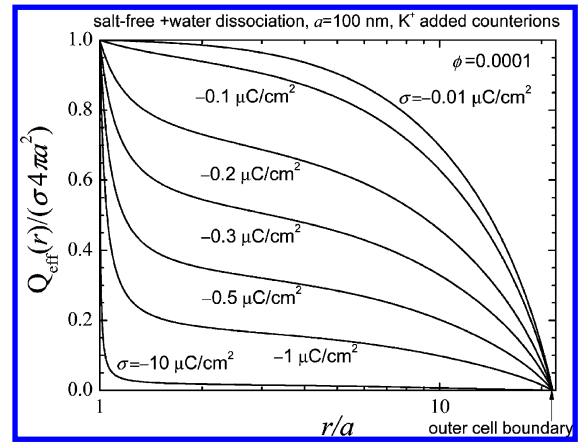

Figure 2. Dimensionless effective charge as a function of the distance from the particle center for a charged spherical particle in a realistic salt-free suspension SFW, at 25 °C as a function of frequency. The surface charge densities σ are indicated. In all cases, the volume fraction is $\phi = 0.0001$, the particle radius is 100 nm, and the added counterions are K^+.

charge. In order to illustrate the occurrence of such accumulation, Figure 2 shows the net or effective charge Q_{eff} as a function of the distance to the particle center, for different surface charge densities. $Q_{eff}(r)$ represents the total charge "seen" at a distance r from the center of the particle, including the charge of the particle itself plus the volume charge density of the double layer integrated from the surface to the r distance. Note that its value will be equal to the particle charge when $r = a$, whereas it is zero at $r = b$, as expected from the electroneutrality of the cell.

It can be observed that the trend of variation changes significantly when the charge density increases: the higher screening effect attained for high charges manifests in a rapid tendency toward zero, to such extent that, above roughly -1 μC/cm^2, a high concentration of counterions in the vicinity of the surface will develop. This is what has been named the counterion condensation effect.

Concerning the frequency dependence of the dynamic mobility in Figure 1, it can be observed that it is mainly controlled by the amount of surface charge and has little dependency on the salt-free model chosen, either pure or realistic ones. At high surface charge, we observe first of all an increase of the mobility around 1−10 kHz, followed by a maximum and a further decrease until a new maximum is attained, and finally a monotonous decrease toward zero. The latter decrease is known to be produced by the above-mentioned inertia of the particle and fluid, which cannot follow the field oscillations at such high frequencies. Interestingly, the higher frequency maximum is rather independent of the salt-free model used (SF, SFW, and SFWC). On the contrary, the lower frequency rise shifts to higher frequencies from the lowest ionic strength (SF) to the highest ionic strength (SFWC). Such a shift is compatible with a Maxwell−Wagner relaxation.[51] The latter observed increase in the mobility is related to the reduction of the induced electric dipole moment (the polarization is hindered when the frequency is increased). Let us mention that the dipole strength below the relaxation frequency is larger the higher the ionic strength; hence the mobility increase will be larger when this dipole is relaxed. Note that using the approximate relation[51]

$$\omega \sim \frac{2D}{L^2} \tag{50}$$

with L being a characteristic length for the process, we estimate that the characteristic length of this MW process in the SFW case is around 600 nm, very close to the estimated double layer thickness in this case (700 nm). Similar conclusions are reached in the other cases. This confirms the MW nature of the low frequency rise, since it is well-known that the double layer thickness controls the relaxation frequency in such kinds of processes.[51]

The inertial decrease following this MW relaxation is interrupted by a second maximum found at higher frequencies as above-described. In a previous paper[28] concerning pure salt-free suspensions, the numerical predictions at high particle charges clearly showed the existence of both a low and a high frequency relaxations. We then admitted the existence of an alpha process (the low frequency one) as a result of the relaxation of the diffusion currents generated by the counterions concentration gradient (accumulation on the right side and depletion on the left for a field directed from left to right, and for cations as counterions) produced by the applied field. This slow process showed some of the features of the classical alpha relaxation in salt-containing systems (particularly the increase of the alpha relaxation frequency upon increasing volume fraction), corroborating our first conclusion. After a careful analysis of those results and the ones shown in this paper, it can be better concluded that

(i) the larger frequency relaxation still maintains its Maxwell−Wagner nature, but it cannot be associated with the double layer relaxation, as it will be shown below;

(ii) the low relaxation process is not of an alpha-type. It is in fact the classical Maxwell−Wagner process associated with the double layer relaxation.

Considering the relatively high relaxation frequency of the larger frequency process, it can be suggested that it operates with a characteristic length much smaller than that of the double layer thickness (which is characteristic of the low frequency Maxwell−Wagner process). Our numerical calculations show that the counterion condensation region for high particle surface charges could perfectly account for that frequency response. In fact, this high-frequency Maxwell−Wagner process only appears if the particle surface charge is high enough. It is no wonder that it has not been detected until recently. Furthermore, there is no reason to neglect its existence in the case of salt-added suspensions as well if the particles are highly charged and the ionic strength is not high. This will be confirmed in the next section when computing the dielectric response for such cases.

The high frequency relaxation can be described as an MW process with a characteristic length of ∼4 nm; this figure can be considered as an indication of the strong packing of counterions in the condensate, as well as a confirmation of its physical reality. Note that when the surface charge density is reduced to around -1 μC/cm^2, the position of the maximum is shifted to lower frequencies, that is, the characteristic dimension of the condensation region is increased, as expected (Figure 2). It is remarkable that both the frequency and the amplitude of this process are independent of the salt free model used, because it is controlled by the surface charge density. It must be noted that when the surface charge is sufficiently low, the maximum disappears, and this is a manifestation of the fact that the condensate is absent because we are below the critical surface charge density necessary for its existence.[23]

The latter feature of the frequency dependence of the mobility is clearly observed in the phase representation (Figure 1b). Note that the minima displayed around 10^8 Hz for high charge densities tend to merge with those associated to the low frequency MW processes, and finally disappear for charge densities below -0.1 μC/cm^2. Nevertheless, the phase of the mobility is less intuitive than its modulus (or its real part) (compare Figures 1a and 1b). For this reason, we will limit our discussions to the behavior of the modulus.

Dielectric Dispersion. As it is well-known, the frequency dispersion of the relative permittivity (ε^*) of the suspensions, being also controlled by the induced dipole moment, should give us information similar to that provided by the dynamic mobility, except for the inertia processes, which are irrelevant for the dielectric behavior.[51] Figure 3 demonstrates that this is indeed the case. Note the presence of two (one) relaxation peaks for high (low) charge densities. Likewise, the high frequency peak, when present, appears at frequencies depending only on the charge density and not on the salt-free model chosen.

Regarding the behavior of the low frequency peak, this is shifted to higher frequencies when we go from SF to SFWC models, in agreement with mobility data, and due again to the conductivity increase associated with SFW and SFWC models as compared to the SF case. It is also noticeable that the low frequency permittivity is reduced when the model is changed from SF suspensions to realistic descriptions including water dissociation and, mainly, CO_2 contamination. This is coherent with our findings concerning the dynamic mobility (Figure 1) and it is a consequence of the reduction of the surface potential at constant surface charge[33] (when the model is changed as described). Equally evident is the increase of the low frequency values of the permittivity when the surface charge is raised. This is easily explained considering that higher surface charges also mean higher ionic concentration in the polarizable atmosphere. The Maxwell−Wagner origin of the relaxations observed

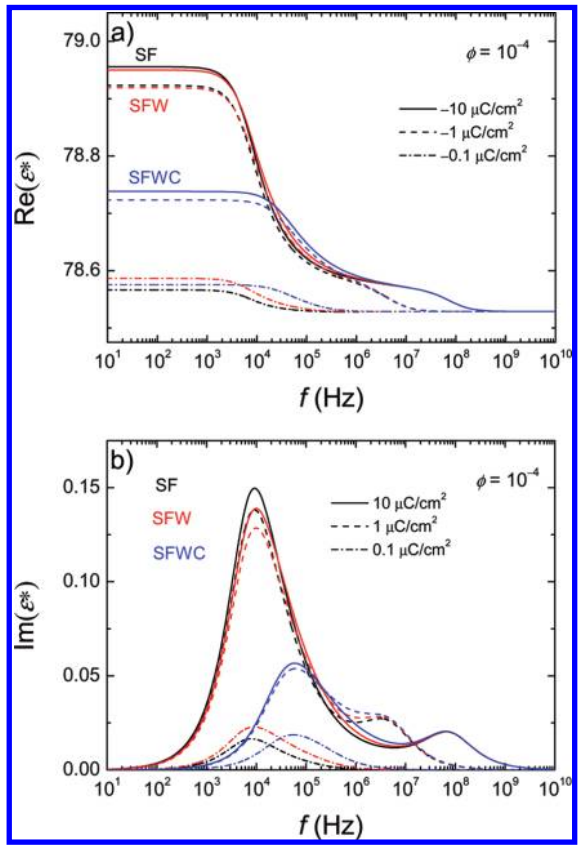

Figure 3. Real (a) and imaginary (b) parts of the relative permittivity of an SF suspension, an SFW suspension, and an SFWC suspension, at 25 °C as a function of frequency. The surface charge densities σ are indicated. Volume fraction: $\phi = 0.0001$; particle radius: $a = 100$ nm; added counterions: H^+.

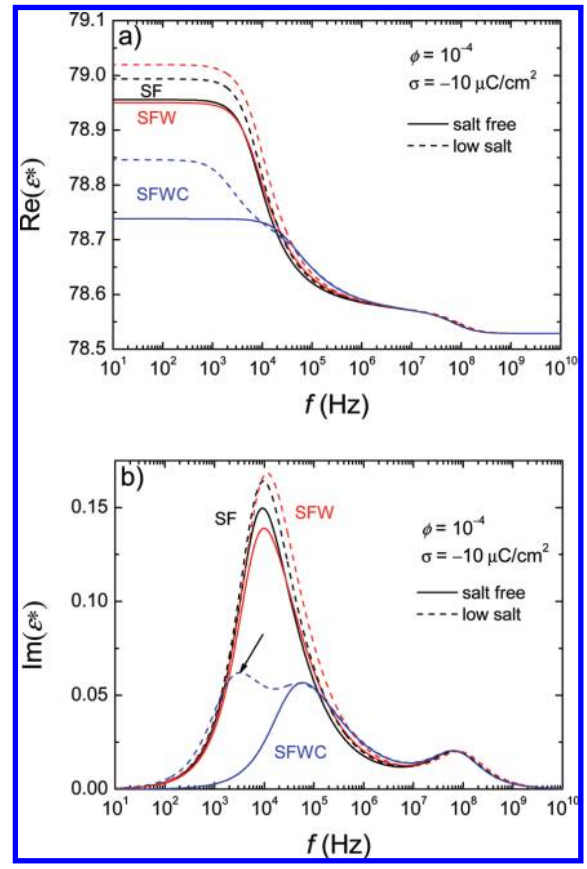

Figure 4. Real (a) and imaginary (b) parts of the relative permittivity of pure (SF) and realistic (SFW, SFWC) salt-free suspensions (solid lines), and of the equivalent low-salt suspensions (dashed lines) (see text), at 25 °C as a function of frequency. Surface charge density: $\sigma = -10$ μC/cm^2. Volume fraction: $\phi = 0.0001$; particle radius: $a = 100$ nm; added counterions: H^+. The arrow indicates the true α relaxation appearing in low-salt conditions, but absent in salt-free systems with otherwise the same properties.

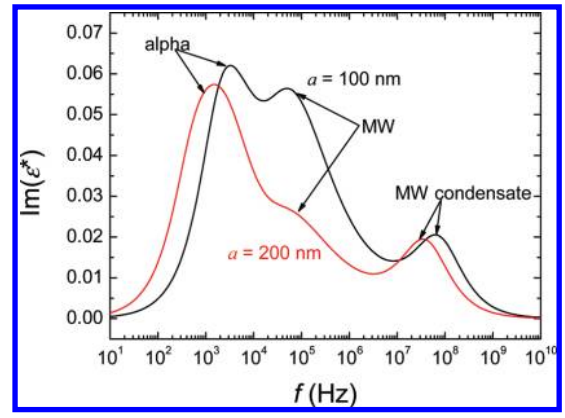

Figure 5. Imaginary part of the relative permittivity of a low-salt suspension for two particle sizes in a HCl solution ($2.23.10^{-6}$ mol/L), at 25 °C as a function of frequency. Zeta potential: $\zeta = -360$ mV. Volume fraction: $\phi = 0.0001$.

in Figure 3 can be confirmed by calculating the permittivity of suspensions in ordinary electrolyte solutions (HCl in our case) with concentration low enough to match the conductivity of the salt-free systems[52] depicted in Figure 4. These suspensions are often called low-salt dispersed systems.[19] Calculations were performed using standard cell models as described in ref 12, taking the zeta potential of the particles in such a way that the surface charge and the DC conductivity are the same as in the salt-free case.[33]

Figure 4 shows the results: the salt-free data are replotted together with the low-salt calculations. The appearance of the low frequency relaxation (true α-process) around 2 kHz is evident in the low-salt case matching the SFWC model. For the SF and SFW choices, the distinction is hindered by the fact that the double layer is so thick that the Maxwell−Wagner and α relaxations occur at very close frequencies, and their corresponding loss peaks appear to merge. Still further confirmation comes from the evaluation of the effect of the particle size on the overall low-salt permittivity spectrum.

Thus, in Figure 5 we display the imaginary component of the permittivity, where we can observe the presence of three relaxation peaks, which change differently when the particle radius is increased from 100 to 200 nm. The lowest-frequency process shifts to lower frequency, the second peak remains essentially unaltered in frequency, and the high frequency relaxation also moves to lower frequencies. These changes are consistent with the picture described above: the lowest frequency process is an α relaxation. As such, its characteristic frequency should change with the inverse square of the dimension of the particle plus its double layer. The middle frequency peak is a Maxwell−Wagner relaxation controlled by the double layer thickness (which is the same for the two curves depicted). Finally, the high frequency peak is also of Maxwell−Wagner origin, and, since it is associated to the counterion condensate, it will be controlled essentially by the surface charge density. Note that the two curves in Figure 5 have been calculated using the same zeta potential, but in such conditions the surface charge density is lower for the higher particle radius. Therefore, the

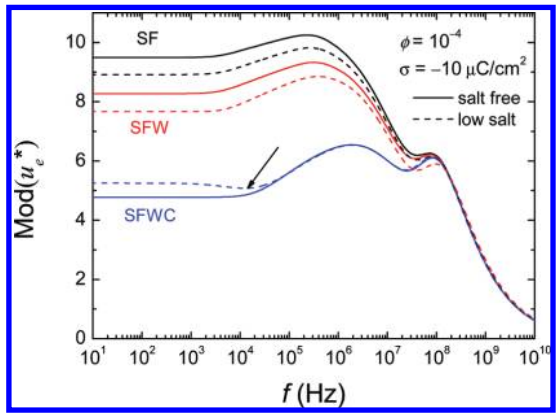

Figure 6. Same as Figure 4 but for the modulus of the dimensionless dynamic electrophoretic mobility.

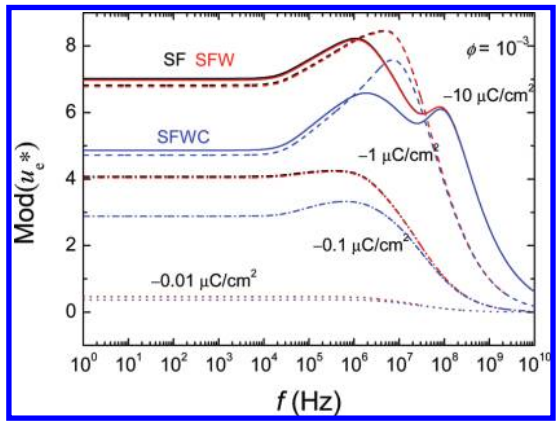

Figure 7. Modulus of the dimensionless dynamic electrophoretic mobility of a spherical particle in a salt-free suspension (SF), and in realistic salt-free suspensions (SFW and SFWC)), at 25 °C as a function of frequency. The surface charge densities σ are indicated. Volume fraction: $\phi = 0.001$; particle radius: $a = 100$ nm; addd counterions: H^+.

peak corresponding to the larger size should appear at lower frequencies, as in fact observed.

We may wonder why no alpha relaxation is observed in the case SFWC, considering that we could think of the carbonic acid as a neutral electrolyte, although a weak one. However, Grosse and Shilov demonstrated that the α relaxation process could be of very little significance, or even inexistent, in solutions of such weak electrolytes.[53]

It is worthwhile to consider whether the same features can be observed in dynamic mobility calculations. With that aim, we have plotted in Figure 6 the modulus of the mobility as a function of frequency for the case of highest surface charge shown in Figure 3. It can be clearly observed that, for all salt-free models, the mobility is frequency independent up to the first increase associated with the first Maxwell−Wagner process. On the contrary, the low-salt calculations show a decrease (indicated by an arrow in Figure 6) at a few kilohertz prior to the above-mentioned rise. Such a decrease is a clear indication of an α relaxation process.[50]

Volume Fraction Effects. In Figures 7−9 (see also Figure 1), we study the effect of the particle volume fraction on the dynamic mobility of a spherical particle in pure and realistic salt-free suspensions. A remarkable result is the volume fraction independence of the highest-frequency Maxwell−Wagner relaxation peak, which we have associated with the relaxation of the counterion condensate at high surface charges. On the contrary, as volume fraction increases for fixed surface charge

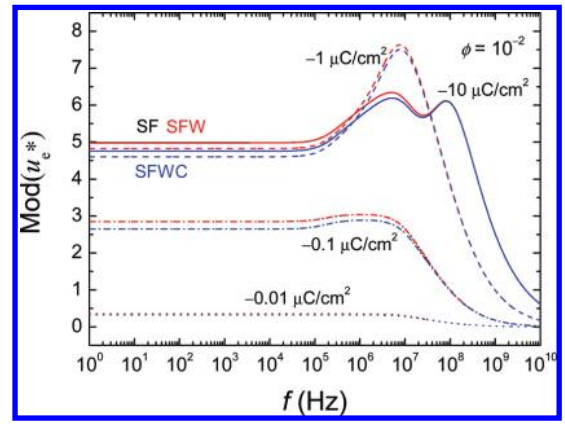

Figure 8. Same as Figure 7 for the volume fraction $\phi = 0.01$.

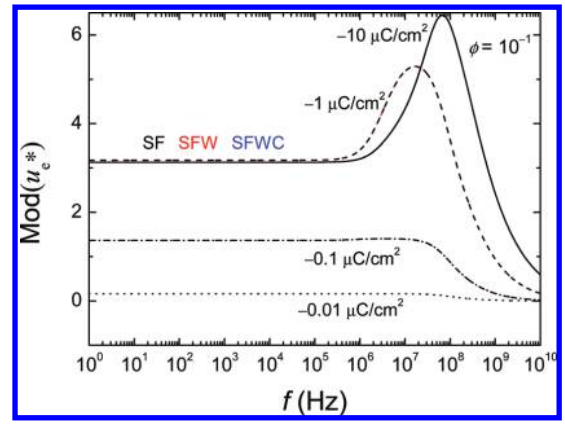

Figure 9. Same as Figure 7 for the volume fraction $\phi = 0.1$.

density, there will be more charges per unit volume in the system, and the double layers will be more compressed. This fact and the diminution of the particle diffusion length with volume fraction, provoke the observed shift of the lowest frequency Maxwell−Wagner peak to larger frequencies. In addition, the latter shift to higher frequencies is larger the larger the ionic strength in the system from pure to realistic salt-free suspensions. Note also that, as volume fraction increases, the roles of ions from water dissociation and CO_2 contamination become less important, as their number is progressively screened by that of the added counterions. This is particularly clear for the highest volume fraction, where no distinction appears between pure and realistic salt-free suspensions (Figure 9).

Finally, for the largest volume fraction and especially for the largest particle surface charge, no separation is found between the two Maxwell−Wagner peaks, as both tend to merge giving the unique high frequency peak observed. Such a merging process is originated by the shift toward higher frequencies of the ordinary MW maximum. This occurs because increasing volume fraction leads to higher concentration of added counterions, and the subsequent increase in conductivity moves the MW relaxation peak to higher frequencies (eq 48). On the contrary, the condensate relaxation remains at the same frequency for a given surface charge.

Conclusions

In this work a cell model is used to derive the dynamic electrophoretic mobility of a spherical particle in pure and realistic salt-free suspensions, the latter including effects such as water dissociation and CO_2 contamination. It is found that, in either pure or realistic salt-free models, the frequency dependence of the dynamic mobility is basically connected to

the presence of one or two Maxwell−Wagner relaxation processes depending on the magnitude of the surface charge, in addition to the high frequency inertia decline. For low surface charge, only one MW process is observed, associated with common double layer relaxation at a few megahertz. If the surface charge is high enough, additional MW relaxation taking place at higher frequencies is observed. This is related to the relaxation of the counterion condensate that develops close to the particle surface for highly charged particles.

In order to reinforce this interpretation of the mobility spectrum, computations of the dielectric response of salt-free suspensions have been performed and compared to results obtained in the case of low-salt suspensions. These have been built using values of the zeta potential and the salt concentration such that the DC conductivity and the surface charge density of the salt-free systems are mimicked. To our knowledge it is the first time that a clear α-process and the above-mentioned two MW processes have been detected simultaneously. Comparison with the corresponding salt-free suspensions has clearly shown the presence of the two MW processes while the α one is missing.

The low frequency mobility is greatly diminished as the ionic strength increases from pure (SF) to realistic (SFW and SFWC) salt-free cases, due to the larger screening associated to the higher ionic strength. Quite interesting, the high frequency MW peak is exactly the same for pure and realistic salt-free cases, because it is linked to the value of the particle surface charge and not to the specific ionic double layer environments.

These corrections should be taken into account for a rigorous comparison with experiments concerning aqueous salt-free suspensions, and we encourage the experimentalists to perform appropriate experiments to analyze the realm of the present corrections. Finally, as volume fraction increases, the difference between pure and realistic salt-free models becomes negligible because of the overwhelming influence of the high concentration of counterions coming from particle surface charging.

Acknowledgment. Financial support for this work by Ministerio de Educación y Ciencia, Spain, Project FIS2007-62737, and Junta de Andalucía, Spain, Projects P08-FQM-03779 and P08-FQM-03993, cofinanced with FEDER funds by the EU, is gratefully acknowledged.

References and Notes

(1) Levine, S.; Neale, G. H. *J. Colloid Interface Sci.* **1974**, *47*, 520.
(2) Levine, S.; Neale, G. H.; Epstein, N. *J. Colloid Interface Sci.* **1976**, *57*, 424.
(3) O'Brien, R. W. *J. Fluid Mech.* **1990**, *212*, 81.
(4) Ohshima, H. *J. Colloid Interface Sci.* **1997**, *188*, 481.
(5) Ohshima, H. *J. Colloid Interface Sci.* **1997**, *195*, 137.
(6) Ohshima, H. *J. Colloid Interface Sci.* **1998**, *208*, 295.
(7) Marlow, B. J.; Fairhurst, D.; Pendse, H. P. *Langmuir* **1998**, *4*, 611.
(8) Ohshima, H. *J. Colloid Interface Sci.* **1999**, *212*, 443.
(9) Ohshima, H.; Dukhin, A. S. *J. Colloid Interface Sci.* **1999**, *212*, 449.
(10) Dukhin, A. S.; Ohshima, H.; Shilov, V. N.; Goetz, P. J. *Langmuir* **1999**, *15*, 3445.
(11) Carrique, F.; Arroyo, F. J.; Delgado, A. V. *J. Colloid Interface Sci.* **2001**, *243*, 351.
(12) Carrique, J.; Arroyo, F. J.; Jiménez, M. L.; Delgado, A. V. *J. Chem. Phys.* **2003**, *118*, 1945.
(13) Ruiz-Reina, E.; Carrique, F.; Rubio-Hernández, F. J.; Gómez-Merino, A. I.; García-Sánchez, J. P. *J. Phys. Chem. B* **2003**, *107*, 9528.
(14) Sood, A. K. *Solid State Phys.* **1991**, *45*, 1.
(15) Medebach, M.; Palberg, T. *J. Chem. Phys.* **2003**, *119*, 3360.
(16) Medebach, M.; Palberg, T. *Colloids Surf., A* **2003**, *222*, 175.
(17) Wette, P.; Schöpe, H. J.; Palberg, T. *Colloids Surf., A* **2003**, *222*, 311.
(18) Medebach, M.; Palberg, T. *J. Phys.: Condens. Matter* **2004**, *16*, 5653.
(19) Palberg, T.; Medebach, M.; Garbow, N.; Evers, M.; Fontecha, A. B.; Reiber, H.; Bartsch, E. *J. Phys.: Condens. Matter* **2004**, *16*, S4039.
(20) Imai, N.; Oosawa, F. *Busseiron Kenkyu* **1952**, *52*, 42.
(21) Oosawa, F. *Polyelectrolytes*; Dekker: New York, 1971.
(22) Ohshima, H. *J. Colloid Interface Sci.* **2002**, *247*, 18.
(23) Ohshima, H. *J. Colloid Interface Sci.* **2002**, *248*, 499.
(24) Ohshima, H. *J. Colloid Interface Sci.* **2003**, *262*, 294.
(25) Ohshima, H. *J. Colloid Interface Sci.* **2003**, *265*, 422.
(26) Ohshima, H. *Colloids Surf., A* **2003**, *222*, 207.
(27) Chiang, C. P.; Lee, E.; He, Y. Y.; Hsu, J. P. *J. Phys. Chem. B* **2006**, *110*, 1490.
(28) Carrique, F.; Ruiz-Reina, E.; Arroyo, F. J.; Delgado, A. V. *J. Phys. Chem. B* **2006**, *110*, 18313.
(29) Shilov, V. N.; Zharkikh, N. I.; Borkovskaya, Y. B. *Colloid J.* **1981**, *43*, 434.
(30) Borkovskaya, Y. B.; Zharkikh, N. I.; Dudkina, L. M. *Colloid J.* **1982**, *44*, 578.
(31) Shilov, V. N.; Zharkikh, N. I.; Borkovskaya, Y. B. *Colloid J.* **1985**, *47*, 645.
(32) Ruiz-Reina, E.; Carrique, F. *J. Phys. Chem. C* **2007**, *111*, 141.
(33) Ruiz-Reina, E.; Carrique, F. *J. Phys. Chem. B* **2008**, *112*, 11960.
(34) Carrique, F.; Ruiz-Reina, E. *J. Phys. Chem. B* **2009**, *113*, 8613.
(35) Ruiz-Reina, E.; Carrique, F. *J. Colloid Interface Sci.* **2010**, *345*, 538.
(36) Ahualli, S.; Delgado, A. V.; Miklavcic, S. J.; White, L. R. *Langmuir* **2006**, *22*, 7041.
(37) Bradshaw-Hajek, B. H.; Miklavcic, S.; White, L. R. *Langmuir* **2008**, *24*, 4512.
(38) Kuwabara, S. *J. Phys. Soc. Jpn.* **1959**, *14*, 527.
(39) O'Brien, R. W.; White, L. R. *J. Chem. Soc., Faraday Trans. 2* **1978**, *74*, 1607.
(40) Ohshima, H.; Healy, T. W.; White, L. R. *J. Chem. Soc., Faraday Trans. 2* **1983**, *79*, 1613.
(41) DeLacey, E. H. B.; White, L. R. *J. Chem. Soc., Faraday Trans. 2* **1981**, *77*, 2007.
(42) Mangelsdorf, C. S.; White, L. R. *J. Chem. Soc., Faraday Trans.* **1998**, *94*, 2441.
(43) Carrique, F.; Ruiz-Reina, E.; Arroyo, F. J.; Jiménez, M. L.; Delgado, A. V. *Langmuir* **2008**, *24*, 2395.
(44) Carrique, F.; Cuquejo, J.; Arroyo, F. J.; Jiménez, M. L.; Delgado, A. V. *Adv. Colloid Interface Sci.* **2005**, *118*, 43.
(45) Lee, E.; Yen, F. Y.; Hsu, J. P. *J. Phys. Chem. B* **2001**, *105*, 7239.
(46) Carrique, F.; Arroyo, F. J.; Delgado, A. V. *J. Colloid Interface Sci.* **2002**, *252*, 126.
(47) Hsu, J. P.; Lee, E.; Yen, F. Y. *J. Phys. Chem. B* **2002**, *106*, 4789.
(48) Cuquejo, J.; Jiménez, M. L.; Delgado, A. V.; Arroyo, F. J.; Carrique, F. *J. Phys. Chem. B* **2006**, *110*, 6179.
(49) O'Brien, R. W.; Jones, A.; Rowlands, W. N. *Colloids Surf., A* **2003**, *218*, 89.
(50) Arroyo, F. J.; Carrique, F.; Ahualli, S.; Delgado, A. V. *Phys. Chem. Chem. Phys.* **2004**, *6*, 1446.
(51) Lyklema, J. *Fundamentals of Interface and Colloid Science: Solid−Liquid Interfaces*; Academic Press: London, 1995; Vol. II.
(52) Carrique, F.; Ruiz-Reina, E. *J. Phys. Chem. B* **2009**, *113*, 10261.
(53) Grosse, C.; Shilov, V. N. *J. Colloid Interface Sci.* **2000**, *225*, 340.

JP102350D